

# Magnetic excitation in a new spin gap compound $\text{Cu}_2\text{Sc}_2\text{Ge}_4\text{O}_{13}$ : Comparison to $\text{Cu}_2\text{Fe}_2\text{Ge}_4\text{O}_{13}$

T. Masuda<sup>1,\*</sup> and G. J. Redhammer<sup>2</sup>

<sup>1</sup>*International Graduate School of Arts and Sciences, Yokohama City University,  
22-2, Seto, Kanazawa-ku, Yokohama city, Kanagawa, 236-0027, Japan<sup>†</sup>*

<sup>2</sup>*Department of Material Science, Division of Mineralogy,  
University of Salzburg, Hellbrunnerstr. 34, Salzburg A-5020, Austria*  
(Dated: March 23, 2022)

The compound  $\text{Cu}_2\text{Sc}_2\text{Ge}_4\text{O}_{13}$  is presented as a new member of the family of weakly coupled spin chain and dimer compounds  $\text{Cu}_2\text{M}_2\text{Ge}_4\text{O}_{13}$ . Magnetic susceptibility, heat capacity, and neutron inelastic scattering measurements reveal that the compound has the same spin dimer component as  $\text{Cu}_2\text{Fe}_2\text{Ge}_4\text{O}_{13}$ . The observed narrow band excitation in bulk measurements is consistent with spin gap behavior. The energy scale of the weakly coupled dimers in the Sc compound is perfectly coincident with that in the Fe compound.

PACS numbers: 75.10.Jm, 75.25.+z, 75.50.Ee

## I. INTRODUCTION

In the last few decades, low-dimensional spin frameworks have played key roles in condensed matter science. Some of the remarkable phenomena on such spin frameworks include high critical temperature superconductivity in doped two-dimensional antiferromagnets,<sup>1,2</sup> exotic superconductivity in spin ladders,<sup>3,4</sup> and multiferroics in frustrated compounds.<sup>5</sup> A fundamental topic from the point of magnetism underlying these phenomena is the ordered or disordered in the ground state. In some spin frameworks, the ground state is strongly disordered by quantum fluctuation and is characterized by associated spin gap excitation. The spin liquid state, on the other hand, is relatively robust with respect to external perturbation, and thus the spin correlation remains short-ranged even at zero temperature. In conventional networks, such as chains or planes with gapless excitation, the ordered states are induced at finite temperatures.

Bicomponent systems combining these distinct spin frameworks have recently been realized experimentally using  $\text{R}_2\text{BaNiO}_5$ ,<sup>6,7</sup>  $\text{Cu}_2\text{Fe}_2\text{Ge}_4\text{O}_{13}$ ,<sup>8</sup> and  $\text{Cu}_2\text{CdB}_2\text{O}_6$ .<sup>9</sup> In the cooperative ordered state of such bicomponent systems, one component is strongly bound to a nonmagnetic singlet state, while the other maintains the usual ordered state. The weakly coupled compound of Cu dimers and Fe chains,  $\text{Cu}_2\text{Fe}_2\text{Ge}_4\text{O}_{13}$ , exhibits two spin excitations with separate energy scales, clearly observable by neutron scattering experiment.<sup>10</sup> In the low-energy range below 10 meV, the excitations are well explained by effectively coupled Fe chains. The dimers behave as media that transfer exchange coupling between Fe chains, and the intradimer interaction can be included in effective interchain coupling. At higher energy, the dispersionless excitation observed at  $\hbar\omega \sim 24$  meV is qualitatively explained by the effect of Cu dimers. The discovery of a new member of the bicomponent compound family has been eagerly awaited in order to continue systematic study of exotic types of ordering.

One of the present authors (G.J.R.) recently identified a new isostructural compound  $\text{Cu}_2\text{Sc}_2\text{Ge}_4\text{O}_{13}$ .<sup>11</sup> The crystal structure is monoclinic, with structural parameters  $a = 12.336(2)$  Å,  $b = 8.7034(9)$  Å,  $c = 4.8883(8)$  Å, and  $\beta = 95.74(2)^\circ$ , and space group  $P2_1/m$ . A schematic drawing of the structure is shown in Fig. 1. The crankshaft chains of  $\text{FeO}_6$  in  $\text{Cu}_2\text{Fe}_2\text{Ge}_4\text{O}_{13}$  are replaced by non-magnetic  $\text{ScO}_6$  chains, and the remnant Cu dimers are separated by  $\text{GeO}_4$  tetrahedra and  $\text{ScO}_6$  chains. All dimers are equivalent. On the basis of this crystallography,  $\text{Cu}_2\text{Sc}_2\text{Ge}_4\text{O}_{13}$  is a candidate for a mono-component system with a single spin-gap framework analogous to that of  $\text{Cu}_2\text{Fe}_2\text{Ge}_4\text{O}_{13}$ . In the present study,  $\text{Cu}_2\text{Sc}_2\text{Ge}_4\text{O}_{13}$  is characterized by a combination of bulk measurements and thermal neutron scattering experiment. Supplemental bulk measurements are also performed on the corresponding Fe compound in order to refine the estimated exchange constants. It is demonstrated that  $\text{Cu}_2\text{Sc}_2\text{Ge}_4\text{O}_{13}$  and  $\text{Cu}_2\text{Fe}_2\text{Ge}_4\text{O}_{13}$  are ideal compounds for the systematic study of bicomponent systems with spin-gap and gapless frameworks.

## II. EXPERIMENTAL DETAILS

A polycrystalline sample of  $\text{Cu}_2\text{Sc}_2\text{Ge}_4\text{O}_{13}$  was prepared by a solid-state reaction route.<sup>11</sup> A high-quality sample was obtained after several regrind and reheat procedures. As the compound exhibits incongruent melting, a single crystal is not available at present. For the Fe compound, a single crystal was obtained by the floating zone method, and 20 mg of the crystal was carefully cut from the rod-shaped bulk crystal so as to ensure that the surface would be free of magnetic impurities. The crystallographic  $c$  direction of these compounds is determined by the edge of a pair of cleavage planes  $\{1\ 1\ 0\}$ . The magnetic susceptibility of both the Sc and Fe compounds were measured under a 1000 Oe field using a commercial SQUID magnetometer (MPMS, Quantum Design

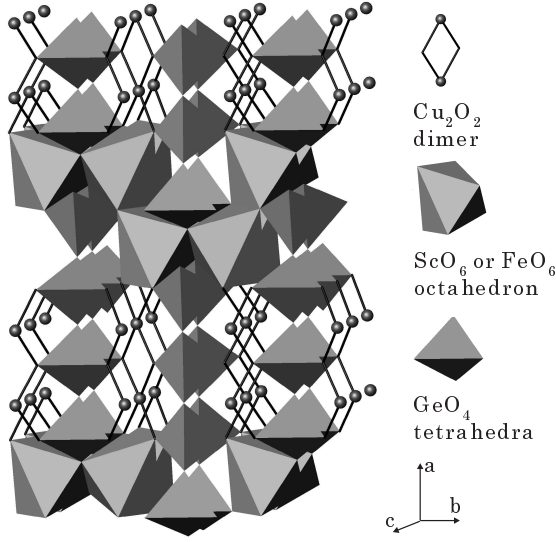


FIG. 1: (Color online) Crystal structure of isostructural compounds  $\text{Cu}_2\text{Sc}_2\text{Ge}_4\text{O}_{13}$  and  $\text{Cu}_2\text{Fe}_2\text{Ge}_4\text{O}_{13}$

Co. Ltd.). Heat capacity measurements were performed using a commercial calorimeter (PPMS, Quantum Design Co. Ltd.). For neutron scattering experiment, 50 g of the Sc polycrystalline sample was placed in an Al can. The neutron inelastic scattering experiment was performed using the PONTA spectrometer at the 5G beamline of the JRR3 JAEA Tokai. Sollar collimation was employed in open - 40' - 40' - 80' configuration with  $E_f = 13.5$  meV, and a pyrolytic graphite filter was inserted after the sample to eliminate contamination from higher harmonics. A closed-cycle helium refrigerator was used to achieve low temperatures. Spurious peaks due to the Sc incoherent scattering, which were accidentally observed in case of  $2k_i = 3k_f$ , is subtracted from all constant- $q$  scans. A vanadium incoherent scan was performed to verify the calculations of instrumental resolution.

### III. RESULTS

The magnetic susceptibility of  $\text{Cu}_2\text{Sc}_2\text{Ge}_4\text{O}_{13}$  after Curie term subtraction is shown in Fig. 2. A broad maximum at 170 K and a dramatic decrease at low temperature are observed. No phase transition was detected down to 2 K. This thermally activated behavior suggests the existence of a spin gap. The heat capacity in the zero field is shown in the inset. The absence of a phase transition was consistently confirmed in these scans.

A series of constant- $q$  scans at 5 K is shown in Fig. 3(a). The scans are shown after linear background subtraction. Well-defined peaks can be observed at energy transfer of 25 meV over all values of  $q$ . The peak width is close to that of the calculated resolution function, and the peak energy of the present compound is coincidence with

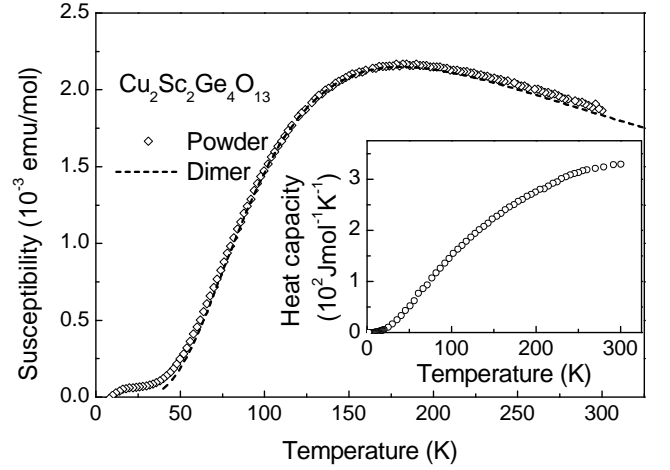


FIG. 2: Magnetic susceptibility of  $\text{Cu}_2\text{Sc}_2\text{Ge}_4\text{O}_{13}$ . Dotted line denotes theoretical calculation (see text). Inset shows heat capacity in zero field.

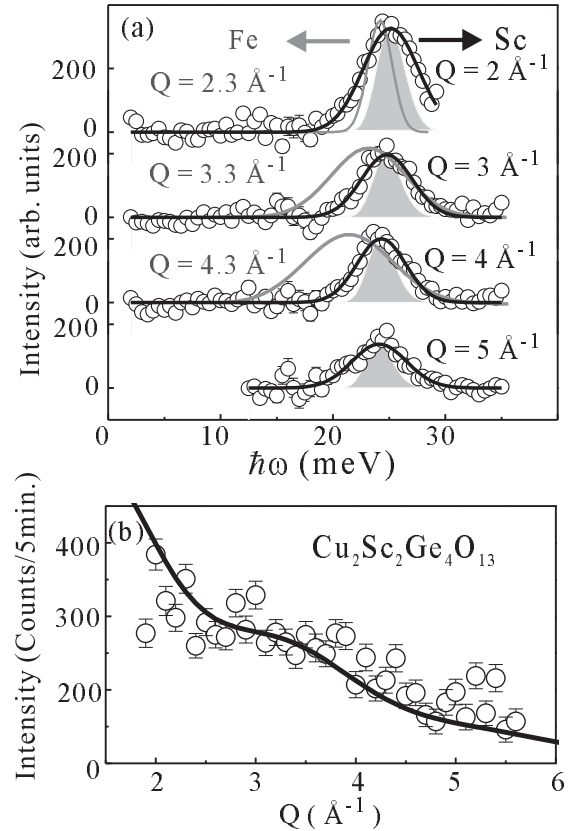


FIG. 3: (a) Constant- $q$  scans at 5 K. Black solid lines denote simple Gaussian fits, shaded areas represent instrumental resolution, and gray lines denote dimer excitation in the Fe compound from Ref. 10. (b) Constant-energy scan at 5 K. Solid lines denotes theoretical calculation (see text).

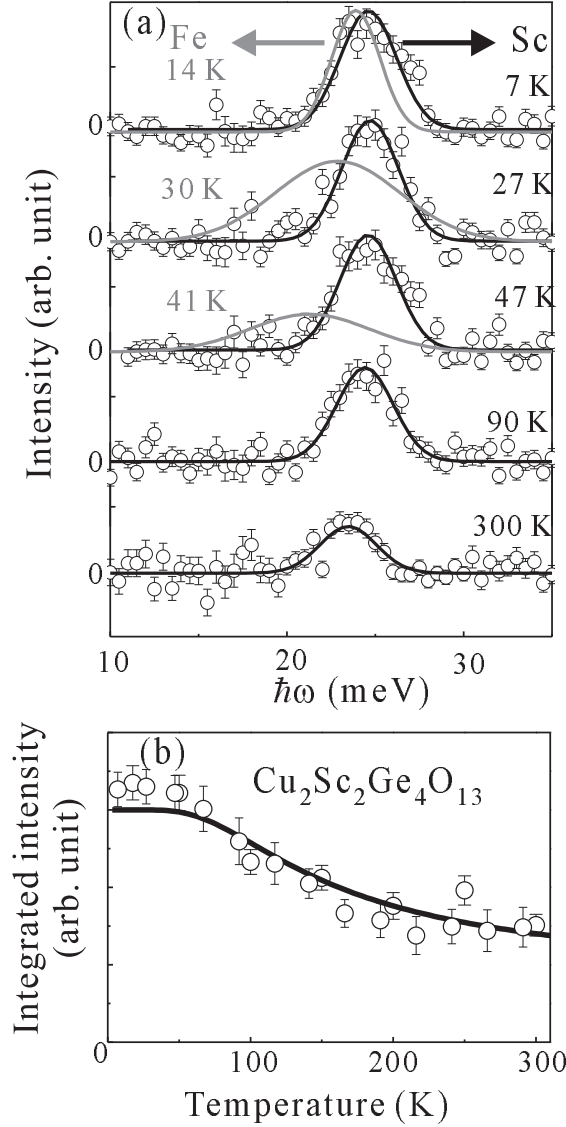


FIG. 4: (a) Temperature scans for Sc compound (open circles) and Fe compound (gray lines),<sup>8</sup> obtained at  $q = 3 \text{ \AA}^{-1}$  and  $q = 2.3 \text{ \AA}^{-1}$ , respectively. Solid lines denote Gaussian fits. (b) Temperature dependence of integrated intensity for  $\text{Cu}_2\text{Sc}_2\text{Ge}_4\text{O}_{13}$ . Solid line denotes theoretical calculation.

that of the corresponding Fe compound.<sup>10</sup> The constant-energy scan at  $\hbar\omega = 25 \text{ meV}$  is shown in Fig. 3(b) after background subtraction. We used the constant- $q$  scan at  $\hbar\omega = 20 \text{ meV}$  as the background. The intensity exhibits a monotonic weakening with increasing  $q$ . The temperature dependence of the energy scan at  $q = 3 \text{ \AA}^{-1}$  is shown in Fig. 4(a). Well-defined peaks with constant width are observable up to 300 K. The temperature dependence of the integrated intensity for the Sc compound is summarized in Fig. 4(b).

The magnetic susceptibility of  $\text{Cu}_2\text{Fe}_2\text{Ge}_4\text{O}_{13}$  is shown in Fig. 5. While the behavior is qualitatively consistent with that seen in the previous study on the Fe com-

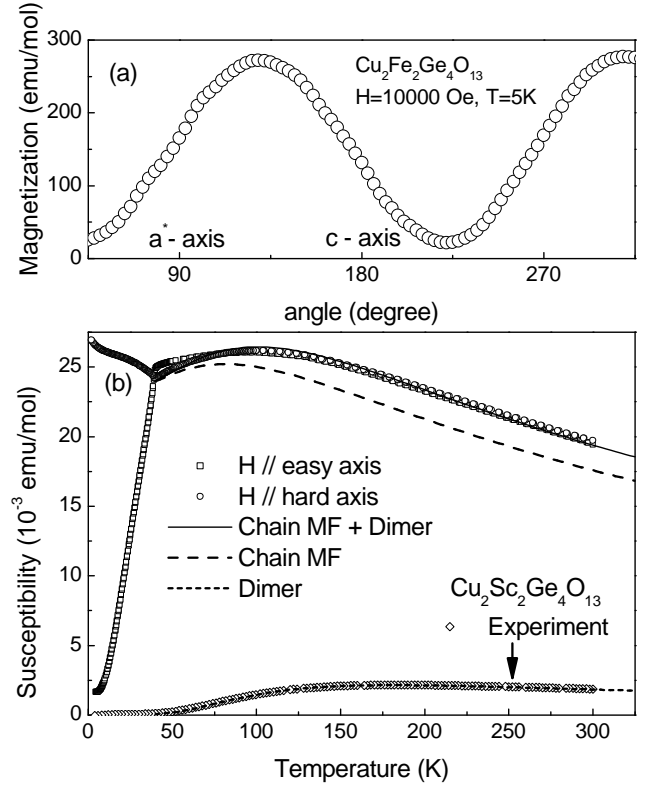


FIG. 5: (a) Angular dependence of magnetization in  $\text{Cu}_2\text{Fe}_2\text{Ge}_4\text{O}_{13}$  ( $180^\circ$  is roughly coincident with crystallographic  $c$  axis). (b) Magnetic susceptibility of  $\text{Cu}_2\text{Fe}_2\text{Ge}_4\text{O}_{13}$  in field oriented parallel to the magnetic easy and hard axes. Solid, dashed, and dotted lines denote theoretical calculations (see text).

pound,<sup>8</sup> the absolute magnitude of the high-temperature susceptibility is approximately 15% lower. As care was taken in the present study to ensure that there would be no magnetic impurities on the freshly cut bulk crystal surface, it is considered that the larger susceptibility results obtained previously were affected by a temperature-independent susceptibility component attributable to magnetic impurities on the surface of the bulk crystal.

Prior to obtaining the present data, the magnetic easy axis was identified by measuring the angular dependence of the magnetization around the  $b$  axis (Fig. 5(a)). Enhanced modulation was observed in the  $a$ - $c$  plane. The  $c$  and  $a^*$  axes approximately correspond to angles of  $180^\circ$  and  $90^\circ$ , respectively. The easy axis was identified by a minima in magnetization located approximately  $45^\circ$  from the  $c$  axis. This result is consistent with the magnetic structure analysis conducted previously for the Fe compound.<sup>8</sup>

The magnetic susceptibility in the easy and hard directions is shown in Fig. 5(b). The marked decrease in susceptibility in the easy direction at  $\lesssim 40 \text{ K}$  is ascribed to the Néel transition. The anisotropic behavior of typical antiferromagnets is clearly observed in the

hard direction. The existence of a single anomaly over the entire temperature region means that the transition is a cooperative ordering in the bicomponent system. In the high-temperature region, enhancement of short-range antiferromagnetic correlation is indicated by the broad maximum around 100 K. As discussed below, the total susceptibility can be explained by the sum of Fe coupled chain and Cu dimer components.

#### IV. ANALYSIS AND DISCUSSION

Consistent with the crystallography, a spin dimer model is employed to describe the magnetic susceptibility of the Sc compound, as given by

$$\chi^{\text{cu}} = \frac{Ng^2\mu_B^2}{k_B T (e^{\frac{J_{\text{Cu}}}{k_B T}} + 3)}. \quad (1)$$

Here  $N$  is the number of Cu ions,  $g$  is gyromagnetic ratio, and  $J_{\text{Cu}}$  is the intradimer interaction. The fit to the data is quite reasonable (dashed line, Fig. 2) with parameters of  $g = 2.02$  and  $J_{\text{Cu}} = 25.(4)$  meV.<sup>14</sup> The dimer energy is close to that of the Cu mode observed in  $\text{Cu}_2\text{Fe}_2\text{Ge}_4\text{O}_{13}$  in the previous neutron scattering study.<sup>8</sup> The spin framework of  $\text{Cu}_2\text{Sc}_2\text{Ge}_4\text{O}_{13}$  is thus equivalent to the Cu dimers in  $\text{Cu}_2\text{Fe}_2\text{Ge}_4\text{O}_{13}$ . The neutron cross-section for spin dimers<sup>12</sup> is given by

$$\frac{d^2\sigma}{d\Omega d\omega} \propto A(T)|f(q)|^2(1 - \frac{1}{qd} \sin qd)\delta(\hbar\omega - J_{\text{Cu}}). \quad (2)$$

The powder average is included in the above formula. An intradimer distance ( $d$ ) of 3.01 Å is adopted here consistent with the crystallography (Fig. 1). Here,  $f(q)$  is the magnetic form factor of  $\text{Cu}^{2+}$  ions and  $A(T)$  is a temperature scaling factor proportional to the thermal distribution of the singlet ground state,  $1/(1+3\exp(-J_{\text{Cu}}/k_B T))$ .

The dispersionless excitations observed in the series of constant- $q$  scans (Fig. 3(a)) is consistent with the description of Eq. (2), and the equation affords a  $J_{\text{Cu}}$  value of 24.(5) meV in agreement with the susceptibility measurements. The monotonic decrease and slight shoulder structure seen in the constant-energy scan is also reproduced well by this formula (Fig. 3(b)). The temperature dependence of integrated intensity (Fig. 4(b)) is further consistent with the calculation using this value of  $J_{\text{Cu}} = 24.(5)$  meV. As the energy width in the constant- $q$  scans appears to be greater than the instrumental resolution (Fig. 3(a)), the dimers are weakly coupled. Interdimer interaction is included by replacing the delta function in Eq. (2) with Gaussian and Lorentzian peak functions. The fitting is reasonable for both cases, affording an estimated intrinsic width of 3.0–5.0 meV. This range represents the band width for Cu dimer excitation in  $\text{Cu}_2\text{Sc}_2\text{Ge}_4\text{O}_{13}$ .

In  $\text{Cu}_2\text{Fe}_2\text{Ge}_4\text{O}_{13}$  the energy scales of Fe and Cu spin frameworks are well separated.<sup>10</sup> The magnetic susceptibility in such a case can thus be described by the sum

TABLE I: Exchange parameters for  $\text{Cu}_2\text{Sc}_2\text{Ge}_4\text{O}_{13}$  and  $\text{Cu}_2\text{Fe}_2\text{Ge}_4\text{O}_{13}$

	$J_{\text{Cu}}$	$J_{\text{Fe}}$	$J'_{\text{Fe}}$
Sc (bulk)	25.(4) meV	-	-
Sc (neutron)	24.(5) meV	-	-
Fe (bulk)	25.(4) meV	1.6(8) meV	0.17(1) meV
Fe (neutron, Ref. 8)	24.(2) meV	1.60(2) meV	0.12(1) meV

of individual contributions. In the lower energy range, the chain mean-field RPA<sup>13</sup> theory is employed for effectively coupled Fe spin chains. Here, Cu dimers between Fe chains are included in the effective interchain coupling. It is assumed that Fe chains on the  $b$  axis are isotropically coupled with a coordination number  $z$  of 4. The uniform magnetic susceptibility is then given by

$$\chi^{\text{Fe}} = \frac{\chi^0}{1 - zJ'_{\text{Fe}}\chi^0} \quad (3)$$

where  $J_{\text{Fe}}$  and  $J'_{\text{Fe}}$  are inchain and interchain interactions and  $\chi^0$  is the susceptibility of isolated classical spin chains.<sup>15</sup> In the high-energy range, the Cu dimer framework dominates the excitation. The interdimer interaction is small as suggested by the dispersionless excitation.<sup>8</sup> It is therefore assumed that the susceptibility can be expressed by the sum of Eqs. (3) and (1).

Fitting of the model to the Fe compound was performed by fixing the Cu dimer parameters to that of the Sc compound. An excellent fit to the data was thus obtained (Fig. 5(b)), yielding parameters of  $J_{\text{Fe}} = 1.6(8)$  meV and  $J'_{\text{Fe}} = 0.17(1)$  meV. These values are consistent with the previous neutron results.<sup>10</sup> The data and associated fitting results show that  $\text{Cu}_2\text{Fe}_2\text{Ge}_4\text{O}_{13}$  is a bicomponent system, and that  $\text{Cu}_2\text{Sc}_2\text{Ge}_4\text{O}_{13}$  has the same dimer component as the Fe compound.

The obtained exchange parameters are summarized in Table I. The perfect coincidence between  $J_{\text{Cu}}$  of the Sc and Fe compounds shows that the Sc compound has the same spin dimer framework as the Fe compound. The remarkable difference between Cu modes in cooperative ordering and the spin liquid can also be observed from the respective temperature dependences. The peak observed for the Fe compound becomes substantially broader with increasing temperature (Fig. 4(a)). This mode appears to be influenced by the magnetic ordering at 40 K.

#### V. CONCLUSION

In summary, a combination of bulk measurements and neutron scattering experiment revealed that  $\text{Cu}_2\text{Sc}_2\text{Ge}_4\text{O}_{13}$  is a mono-component compound of  $\text{Cu}_2\text{Fe}_2\text{Ge}_4\text{O}_{13}$ . All data were consistently explained by a weakly coupled dimer model. The perfect coincidence in the values of  $J_{\text{Cu}}$  demonstrates that  $\text{Cu}_2\text{M}_2\text{Ge}_4\text{O}_{13}$

( $M = \text{Fe}$  and  $\text{Sc}$ ) is a rare experimental realization of cooperative ordering and an associated spin liquid state.

### Acknowledgments

The authors express their great appreciation to R. Jin and B. C. Sales for heat capacity measurements, and A. Zheludev for fruitful discussion in the early stage of this study. The technical help of M. Matsuura, S. Watan-

abe, and K. Hirota in neutron scattering experiment is also gratefully acknowledged. This work was supported by a grant under the 2005 Strategic Research Project (#W17003 and #K17028) of Yokohama City University, Japan, and by a grant to G. J. R from the *Fond zur Förderung der wissenschaftlichen Forschung* (FWF), Austria (#R33-N10). This work was also partially supported by Oak Ridge National Laboratory (ORNL) funding under Contract No. DEAC05-00OR22725 (U. S. Department of Energy).

---

\* tmasuda@yokohama-cu.ac.jp

† Previous address: Condensed Matter Science Division, Oak Ridge National Laboratory, Oak Ridge, TN 37831-6393, USA

<sup>1</sup> J. G. Bednorz and K. A. Müller, Z. Phys. B **64**, 189 (1986).

<sup>2</sup> Y. Tokura, H. Takagi, and S. Uchida, Nature **337**, 345 (1989).

<sup>3</sup> E. Dagotto, J. Riera, and D. Scalapino, Phys. Rev. B **45**, 5744 (1992).

<sup>4</sup> M. Uehara, T. Nagata, J. Akimitsu, H. Takahashi, N. Môri, and K. Kinoshita, J. Phys. Soc. Jpn. **65**, 12199 (1996).

<sup>5</sup> G. Lawes, A. B. Harris, T. Kimura, N. Rogado, R. J. Cava, A. Aharony, O. Entin-Wohlman, T. Yildirim, M. Kenzelmann, C. Broholm, et al., Phys. Rev. Lett. **95**, 087205 (2005).

<sup>6</sup> A. Zheludev, E. Ressouche, S. Maslov, T. Yokoo, S. Raymond, and J. Akimitsu, Phys. Rev. Lett. **80**, 3630 (1998).

<sup>7</sup> A. Zheludev, J. Hill, and D. Buttrey, Phys. Rev. B **54**, 7216 (1996).

<sup>8</sup> T. Masuda, A. Zheludev, B. Grenier, S. Imai, K. Uchinokura, E. Ressouche, and S. Park, Phys. Rev. Lett. **93**, 077202 (2004).

<sup>9</sup> M. Hase, M. Kohno, H. Kitazawa, O. Suzuki, K. Ozawa, G. Kido, M. Imai, and X. Hu, Phys. Rev. B **72**, 172412 (2005).

<sup>10</sup> T. Masuda, A. Zheludev, B. Sales, S. Imai, K. Uchinokura, and S. Park, Phys. Rev. B **72**, 094434 (2005).

<sup>11</sup> G. J. Redhammer and G. Roth, J. Solid State Chem. **177**, 2714 (2004).

<sup>12</sup> A. Furrer and H. U. Gudel, J. Mag. Mag. Mater. **14**, 256 (1979).

<sup>13</sup> D. J. Scalapino, Y. Imry, and P. Pincus, Phys. Rev. B **11**, 2042 (1975).

<sup>14</sup> In this paper the exchange constants  $J$ 's are defined by  $H = J \sum_i \mathbf{S}_i \cdot \mathbf{S}_{i+1}$ .

<sup>15</sup> M. E. Fisher, Am. J. Phys. **32**, 343 (1964).